Published in final edited form as:

Am J Sports Med. 2016 March ; 44(3): 652–663. doi:10.1177/0363546515621285.

Abnormal Mechanical Loading Induces Cartilage Degeneration by Accelerating Meniscus Hypertrophy and Mineralization After ACL Injuries In Vivo

Guoqing Du, MD, PhD[*,†,‡], **Hongsheng Zhan, MD, PhD**[*,†], **Daofang Ding, PhD**[*,†], **Shaowei Wang, MD**[‡,§], **Xiaochun Wei, MD, PhD**[§], **Fangyuan Wei, MD, PhD**[||], **Jianzhong Zhang, MD**[||], **Bahar Bilgen, PhD**[‡,¶], **Anthony M. Reginato, MD, PhD**[#], **Braden C. Fleming, PhD**[‡], **Jin Deng, MD**[**], and **Lei Wei, MD, PhD**[‡,§,††]

[*]Shi's Center of Orthopedics and Traumatology, Shuguang Hospital, Shanghai University of Traditional Chinese Medicine, Shanghai, China

[†]Institute of Traumatology & Orthopedics, Shanghai Academy of Traditional Chinese Medicine, Shanghai, China

[‡]Department of Orthopaedics, Rhode Island Hospital, Warren Alpert Medical School of Brown University, Providence, Rhode Island, USA

[§]Department of Orthopaedics, The Second Hospital, Shanxi Medical University, Taiyuan, China

[||]Foot and Ankle Orthopaedic Surgery Center, Beijing Tongren Hospital, Capital Medical University, Beijing, China

[¶]Providence VA Medical Center, Providence, Rhode Island, USA

[#]Division of Rheumatology, Rhode Island Hospital, Warren Alpert Medical School of Brown University, Providence, Rhode Island, USA

[**]Department of Orthopaedics, Affiliated Hospital of Guiyang Medical University, Guiyang, China

Abstract

[††]Address correspondence to Lei Wei, MD, PhD, Department of Orthopaedics, Rhode Island Hospital, Warren Alpert Medical School of Brown University, 1 Hoppin Street, Suite 402A, Providence, RI 02903, USA (lei_wei@brown.edu).

G.D. and H.Z. contributed equally to this article and are co-first authors.

Investigation performed at the Department of Orthopaedics, Rhode Island Hospital, Warren Alpert Medical School of Brown University, Providence, Rhode Island, USA

One or more of the authors has declared the following potential conflict of interest or source of funding: The project was supported by grant R01AR059142 from the National Institutes of Health (NIH)/National Institute of Arthritis and Musculoskeletal and Skin Diseases; Institutional Development Award P20GM104937 from the NIH/National Institute of General Medical Sciences; grants 81473702, 8150150824, 81201435, 81071495, 81171676, and 31271033 from the National Natural Science Foundation of China; and grants 81572098 GJHZ20130418150248986, JCYJ201304021019 26968, and Career Development Award Number 5IK2RX000760 from the Rehabilitation Research and Development Service, Office of Research and Development, United States Department of Veterans Affairs.

Background—Although patients with an anterior cruciate ligament (ACL) injury have a high risk of developing posttraumatic osteoarthritis (PTOA), the role of meniscus hypertrophy and mineralization in PTOA after an ACL injury remains unknown.

Purpose/Hypothesis—The purpose of this study was to determine if menisci respond to abnormal loading and if an ACL injury results in meniscus hypertrophy and calcification. The hypotheses were that (1) abnormal mechanical loading after an ACL injury induces meniscus hypertrophy and mineralization, which correlates to articular cartilage damage in vivo, and (2) abnormal mechanical loading on bovine meniscus explants induces the overexpression of hypertrophic and mineralization markers in vitro.

Study Design—Controlled laboratory study.

Methods—*In vivo guinea pig study (hypothesis 1):* Three-month-old male Hartley guinea pigs (n = 9) underwent ACL transection (ACLT) on the right knee; the left knee served as the control. Calcification in the menisci was evaluated by calcein labeling 1 and 5 days before knee harvesting at 5.5 months. Cartilage and meniscus damage and mineralization were quantified by the Osteoarthritis Research Society International score and meniscus grade, respectively. Indian hedgehog (Ihh), matrix metalloproteinase–13 (MMP-13), collagen type X (Col X), progressive ankylosis homolog (ANKH), ectonucleotide pyrophosphatase/phosphodiesterase–1 (ENPP1), alkaline phosphatase (ALP), inorganic pyrophosphate (PPi), and inorganic phosphate (Pi) concentrations were evaluated by immunohistochemistry and enzyme-linked immunosorbent assay. *In vitro bovine meniscus explant study (hypothesis 2):* Bovine meniscus explants were subjected to 25% strain at 0.3 Hz for 1, 2, and 3 hours. Cell viability was determined using live/dead staining. The levels of mRNA expression and protein levels were measured using real-time quantitative reverse transcription polymerase chain reaction and Western blot after 24, 48, and 72 hours in culture. The conditioned medium was collected for sulfated glycosaminoglycan (GAG) release and Pi/PPi assay.

Results—*In vivo guinea pig study:* Meniscus size and area as well as intensity of meniscus calcification were significantly increased in the ACLT group compared with the control group. Both calcified area and intensity were correlated with cartilage damage in the ACLT group (meniscus calcified area: $r = 0.925$, $P < .0001$; meniscus calcified intensity: $r = 0.944$, $P < .0001$). Ihh, MMP-13, Col X, ANKH, ENPP1, and ALP expression were increased in the ACLT group compared with the control group. The Pi level and Pi/PPi ratio increased by 63% and 42%, respectively, in the ACLT group compared with the control group. *In vitro bovine meniscus explant study:* Cell death was found in the superficial zone of the bovine meniscus explants after loading for 3 hours. The mRNA expression and protein levels of MMP-13, ANKH, ENPP1, and ALP were up-regulated in all 3-hour loaded samples. The Pi/PPi ratio and sulfated GAG content in the culture medium were increased in the 3-hour loaded group.

Conclusion—Meniscus hypertrophy and mineralization correlated to cartilage degeneration after ACL injuries.

Clinical Relevance—The study data suggest that the suppression of meniscus hypertrophy and calcification may decrease the risk of PTOA after ACL injuries.

Keywords

abnormal mechanical loading; cartilage degeneration; meniscus hypertrophy and mineralization; ACL injury

Knee joint stability is provided by multiple anatomic structures, such as ligaments, tendons, and the meniscus. Among these, the anterior cruciate ligament (ACL) plays a crucial role in guiding knee motion while maintaining knee stability in multiple planes.[30,31] An ACL injury places the patient at a higher risk for the development of posttraumatic osteoarthritis (PTOA).[32,34] After an ACL injury, ACL reconstruction is generally recommended for young patients; however, whether surgery can appreciably reduce the risk of premature PTOA remains controversial.[1,9] The molecular mechanisms behind the onset and development of PTOA in ACL transection (ACLT) also remain inconclusive.

Osteoarthritis (OA) is a disease of the whole joint that involves the meniscus, synovium, articular cartilage, ligaments, tendons, and subchondral bone. Changes in any these structures may contribute to the early development of knee PTOA after an ACL injury.[10,13,15,20] Among these, the meniscus is a specialized tissue that plays a vital role in load transmission, shock absorption, and joint stability.[25,36] A significant increase in meniscus loading was observed long term after ACLT.[3] Thus, the meniscus appears to play a primary role in the early development of knee PTOA after an ACL injury. Although meniscus damage is implicated in the development of PTOA,[24] relatively few studies have directly determined how the meniscus changes in accordance with an ACL injury in the long term.

Previous studies have shown that abnormal compressive loads induce meniscus cell damage and matrix degradation in both in vitro and in vivo models[4,17] and cartilage damage in human samples.[27] However, it is difficult to gain insight into the injury response of meniscus tissue and the correlation between meniscus degeneration and the severity of cartilage damage from imaging studies alone. Collective evidence implicates that pathological meniscus mineralization, which may alter the biomechanical properties of load transmission, shock absorption, and joint stability of the meniscus, is potentially an important contributory factor in the development of primary OA in humans.[24,37] The relationship between ACL injuries and meniscus calcification is relatively unknown and is the focus of this investigation.

The objective of this study was to test the effects of abnormal mechanical loading on meniscus hypertrophy and mineralization. Our hypotheses were that (1) abnormal mechanical loading after an ACL injury induces meniscus hypertrophy and mineralization, which correlates to articular cartilage damage in vivo, and (2) abnormal mechanical loading on bovine meniscus explants induces the overexpression of hypertrophic and mineralization markers in vitro. Our study had 2 parts: to test our first hypothesis, we employed an in vivo ACLT OA model in guinea pigs, and to test our second hypothesis, we used an in vitro model to deliver cyclic loading on bovine meniscus explants to detect the expression of hypertrophy and mineralization markers.

METHODS

In Vivo Guinea Pig Study

Animals—Approval for the animal experiments was obtained from the Institutional Animal Care and Use Committee at Rhode Island Hospital. Three-month-old male Hartley guinea pigs (n = 9) were purchased from Elm Hill Labs. All animals underwent ACLT on the right knee, while the contralateral ACL-intact knee served as the control (left knee). These animals were euthanized 10 weeks after surgery (age, 5.5 months) for specimen collection.

In Vivo Calcein Labeling and Rate of Pathological Matrix Calcification—To detect pathological matrix calcification in the meniscus, calcein (DCAF; Merck) was subcutaneously injected (30 mg/kg body weight in 0.3 mL 0.15 M NaCl containing 2% $NaHCO_3$/animal) 1 and 5 days before the animals were sacrificed.[41] Calcein is a fluorescent label that binds to calcium and is incorporated into growing calcium carbonate crystals to detect calcification during new bone formation.[38]

Histology—After the animals were euthanized, the menisci and proximal tibial plateau of the right (ACLT) and left (control) knees were individually harvested from the animals, and the width of the menisci from the medial meniscus to the lateral meniscus and meniscus length were measured with a ruler. The menisci and proximal tibial plateaus (n = 6) were then immersed in 10% formalin for 72 hours separately. The proximal tibial plateaus were decalcified in 20% ethylenediaminetetraacetic acid (EDTA) solution, while the menisci were processed without decalcification. The specimens were embedded in a single block of Paraplast X-tra (Thermo Fisher Scientific), and 6-μm meniscus and coronal tibia cross-sections were mounted on slides. The amount of pathological matrix calcification in the meniscus was determined by fluorescence microscopy. Alizarin Red and von Kossa staining were also used to evaluate the mineralization of the meniscus. The area and intensity of calcification were determined using HIS-Elements AR software (Nikon). The severity of cartilage damage was determined by the Osteoarthritis Research Society International (OARSI) histological score after the slides were stained using safranin O/Fast Green,[22] and the severity of meniscus damage was graded grossly.[36] Three independent blinded observers scored each section. The association between the area and intensity of meniscus calcification and the severity of cartilage damage was established using regression analysis.

Immunohistochemistry—Meniscus sections 6 μm thick were collected on positively charged glass slides (Thermo Fisher Scientific) to detect the expression of several markers related to hypertrophy and mineralization: matrix metalloproteinase–13 (MMP-13), collagen type X (Col X), Indian hedgehog (Ihh), interleukin-1 (IL-1), progressive ankylosis homolog (ANKH), ectonucleotide pyrophosphatase/phosphodiesterase–1 (ENPP1), and alkaline phosphatase (ALP). The sections were dried on a hot plate to increase tissue adherence. Immunohistochemistry was performed using the 3,3′diaminobenzidine (DAB) Histostain–streptavidin-peroxidase (SP) Immunohistochemistry Kit (Zymed Laboratories/Invitrogen). Sections were deparaffinized and rehydrated using conventional methods. Endogenous peroxidase was blocked by treating the sections with 3% hydrogen peroxide in methanol (Sigma-Aldrich) for 30 minutes. The sections were digested with 5 mg/mL hyaluronidase in

phosphate-buffered saline (PBS; Sigma-Aldrich) for 20 minutes and then incubated with specific antibodies against Ihh (Santa Cruz Biotechnology), MMP-13 (Santa Cruz Biotechnology), Col X (Developmental Studies Hybridoma Bank, University of Iowa), IL-1 (Santa Cruz Biotechnology), ALP (NovusBio), ENPP1 (NovusBio), and ANKH (Abcam), respectively, at 4°C overnight. After the sections were treated sequentially with biotinylated secondary antibody and SP conjugate (Zymed Laboratories/Invitrogen), they were developed in DAB chromogen (Zymed Laboratories/Invitrogen). The sections were counterstained with hematoxylin (Zymed Laboratories/Invitrogen). Photomicrographs were taken with a Nikon Ri1 microscope. Percentages of positive staining for MMP-13, Col X, Ihh, IL-1, ANKH, ENPP1, and ALP from the ACLT and contralateral menisci were semiquantified using Image-Pro Plus 7.0 software (Media Cybernetics), as reported previously.[47] The contralateral knees were used as an internal control. A mean value from 3 independent measurements was calculated for statistical analysis.

Inorganic Pyrophosphate (PPi) and Inorganic Phosphate (Pi)—The menisci of the right (ACLT) and left (control) knees were lysed using the complete Lysis-M kit (#0471 9956001; Roche) (n = 3). The concentrations of PPi and Pi in solution were detected by enzyme-linked immunosorbent assay (ELISA) using the EnzChek Pyrophosphate Assay Kit (E-6645; Molecular Probes) and EnzChek Phosphate Assay Kit (E-6646; Molecular Probes), respectively, following manufacturer instructions using 60-μL lysed samples. The reaction mixtures were incubated for 30 minutes at 22°C, and then the absorbance was read at 360 nm.

In Vitro Bovine Meniscus Explant Study

Cyclic Impact Loading and Culture—The numbers of animals, joints, menisci, explants, and experimental designs in the bovine meniscus explant study are shown in Figure 1A. Medial and lateral menisci were isolated from three 2-year-old mature bovine knees that were procured from a local abattoir. Meniscus disks from each bovine knee were excised from the inner third of the meniscus using a 4 mm–diameter biopsy punch. Each explant was cut perpendicular to the femoral surface of the meniscus to preserve as much of the superficial surface as possible. Each specimen was 3 mm thick (Figure 1B, a–c). A total of 180 explants from the 3 animals were used for the study: each experiment required 60 explants (from 1 animal, 2 knee joints including medial/lateral meniscus) that were randomized to the different experimental groups (no loading, 1 hour, 2 hours, and 3 hours of loading groups) (Figure 1B). The meniscus explants were subjected to cyclic loading by indenting to 25% strain at 0.3 Hz for 1 hour, 2 hours, and 3 hours (Figure 1B). This protocol was selected based on previous reports that 25% strain exceeds the normal strain experienced by menisci during physiological loading.[40,49] The explants were compressed individually in an unconfined culture medium chamber installed in a computer-controlled loading device as previously described.[5] The unloaded control specimens were cultured in the same incubator. During each load cycle, the maximum peak-to-peak strain amplitude (25% of the sample thickness) was maintained for 10 seconds, and then the platen returned to the starting position (Figure 1B, d–f). After compression, the explants were incubated in 1-mL fresh culture medium with 10% fetal bovine serum at 37°C and 5% CO_2. The samples

were randomized into 3 groups and were collected after 24, 48, and 72 hours and stored at −80°C for gene and protein expression analysis.

Cell Viability—Three explants in every group were immediately assayed for cell viability after loading for 1, 2, and 3 hours. Three freeze-thawed cycles of the meniscus were used as a positive cell death control. Cell viability was evaluated by a combination of propidium iodide (PI), which is permeable only to dying cells with damaged plasma membranes (red), and fluorescein diacetate (FDA), which is permeable to and metabolized by live cells (green).[11] The meniscus explants were immersed in 40 ug/mL PI (Molecular Probes/Invitrogen) and 1 uM FDA (Molecular Probes/Invitrogen) for 10 minutes before being observed. Sections were viewed under a fluorescence microscope (Ri1; Nikon).

Measurements of Glycosaminoglycan (GAG) Release—Cumulative GAG concentration in the culture supernatant was determined photometrically using the dimethylmethylene blue dye assay with bovine chondroitin sulfate as a standard control at a wavelength of 525 nm, as previously reported.[23]

Real-Time Quantitative Reverse Transcription Polymerase Chain Reaction (RT-qPCR)—The mRNA levels associated with mineralization, including ANKH, ENPP1, and ALP, were quantified by RT-qPCR. Total RNA was isolated from 24-, 48-, and 72-hour culture samples after 3 hours of loading with the RNeasy isolation kit (Qiagen). We tested the 3-hour loaded samples because cell death was only observed in the superficial zone of the 3-hour loaded samples. Then, 1 μg of total RNA was transcribed into cDNA by using the iScript cDNA synthesis kit (Bio-Rad Laboratories), and 50 ng/μL of the resulting cDNA was used as the template to quantify the relative content of mRNA by using the QuantiTect SYBR Green PCR kit (Qiagen) with the DNA Engine Opticon 2 Continuous Fluorescence Detection System (MJ Research). The primers were designed by using Primers Express software (BioTools):

Bos taurus ANKH forward (sense) primer:

GGCCTTCCTGTATCTTGCTG

ANKH reverse (antisense) primer:

AGGATAGGATGGGGATGAGC

Bos taurus ENPP1 forward (sense) primer:

AGGGTCGCTGTTTTGAGAGA

ENPP1 reverse (antisense) primer:

TCTCCCTTGTCCTTGCAGTC

Bos taurus ALP forward (sense) primer:

AACTCTGCGCAGGATTGGAA

ALP reverse (antisense) primer:

CAGGTACCGATAGCCAGCAG

18S rRNA forward (sense) primer:

CGGCTACCACATCCAAGGAA

18S rRNA reverse (antisense) primer:

GCTGGAATTACCGCGGCT

The 18S rRNA was amplified as the internal control. The cycle threshold values for target genes were measured and calculated with computer software (MJ Research). Relative transcript levels were calculated as $x = 2^{-\Delta\Delta Ct}$ in which ΔΔCt = ΔCt E − ΔCt C, ΔCt E = Ctexp − Ct18S, and ΔCt C = CtCCt − 18S.

Western Blot—The protein levels of MMP-13 and ANKH were determined by Western blot. Total protein was extracted by homogenization with the complete Lysis-M kit (No. 04719956001; Roche) from bovine menisci and quantified by the BAC Protein Assay Kit (Pierce). Equal amounts of protein lysates were separated by sodium dodecyl sulfate–polyacrylamide gel electrophoresis (SDS-PAGE) and transferred to nitrocellulose membranes for immunoblot analysis and stained with specific primary antibodies. The following primary antibodies were used: MMP-13 antibody (H-230, Lot D1113; Santa Cruz Biotechnology) and ANKH antibody (ab90104; Abcam). Fluorescence-labeled secondary antibodies were detected with a fluorescence scanner (Odyssey; LI-COR Biosciences). Band densities were quantified using Image Acquisition and Analysis Software (UVP). Parallel gels were prepared for Coomassie Blue staining to confirm equal loading of the samples as described.[43] Equal amounts of protein were electrophoresed in 10% SDS-PAGE, and the gel was prefixed in 50% MeOH, 10% HoAC, and 40% H_2O for 30 minutes and then stained with 0.25% Coomassie Brilliant Blue R-250 (Bio-Rad Laboratories) in the above solution for 4 hours. The gel was destained in 5% MeOH, 7.5% HoAC, and 87.5% H_2O until the background was clear. The destained gel was stored in 7% HoAC, and a photograph was taken using a Canon camera (SD-1000; Canon Inc).

Quantified PPi and Pi—The culture medium was collected from the control and 3-hour loaded groups cultured after 24, 48, and 72 hours after loading. Cumulative PPi and Pi release into the culture medium were determined by ELISA using the EnzChek Pyrophosphate Assay Kit (E-6645; Molecular Probes) and EnzChek Phosphate Assay Kit (E-6646; Molecular Probes), respectively. The 60-μL medium from each group was analyzed for PPi and Pi concentrations according to manufacturer instructions. The reaction mixtures were read at 360-nm absorbance.

Statistical Analysis

Data are reported as mean ± SD. Two-tailed paired *t* tests were used to compare the size, area, and intensity of meniscus calcification and the damage scores of cartilage and menisci between the ACLT group and control group. Associations between the area and intensity of meniscus calcification and the severity of cartilage damage were determined using correlation analysis. The GAG content in the culture medium and mRNA and protein levels associated with hypertrophy and/or mineralization in the 3-hour loaded and no loading control groups after being cultured for 24, 48, and 72 hours were also compared using 2-

tailed paired *t* tests. Statistical significance was determined at $P < .05$. Statistical analyses were performed using SPSS software (v18.0; IBM Corp).

RESULTS

In Vivo Guinea Pig Study

ACL Injury Resulted in Meniscus Hypertrophy and Accelerated Pathological Matrix Calcification—The meniscus length and width from the medial meniscus to the lateral meniscus were significantly increased in the ACLT group (mean, 15.34 ± 2.03 mm and 10.77 ± 3.26 mm, respectively) compared with the control group (mean, 12.81 ± 2.44 mm and 8.11 ± 2.26 mm, respectively) ($P < .05$) (Figure 2A).

A significant increase in pathological matrix calcification as measured by calcein labeling was detected in whole meniscus tissue (Figure 2B, a and d) and cross-section slides (Figure 2B, b, c, e, and f). ACLT accelerated the area and intensity of pathological matrix calcification in meniscus tissue compared with the control group ($P < .05$) (Figure 2B, g and h).

ACL Injury Accelerated Meniscus Calcification and Was Correlated With Cartilage Damage—Strong Alizarin Red and von Kossa staining (Figure 3A) were detected in the ACLT group compared with the control group. The area and intensity of meniscus calcification were significantly increased by 125% and 120%, respectively, in the ACLT group compared with the control group ($P < .05$) (Figure 3A, g and h).

Histological analysis confirmed severe meniscus (Figure 3B, a and b) and cartilage (Figure 3B, c and d) damage in the ACLT group. The ACLT group had significant clefts and a severe loss of proteoglycan staining at the edge of menisci. Likewise, structural clefts and loss of proteoglycan staining were observed at the superficial, middle, and deep zones of the articular cartilage. In contrast, the control group had minimal meniscus and cartilage damage other than mild proteoglycan loss. The meniscus damage grade (Figure 3B, e) and OARSI score assessing cartilage damage (Figure 3B, f) were significantly increased by 3-fold and 13-fold, respectively, in the ACLT group when compared with the control group ($P < .05$). Significant correlations were found between the area and intensity of meniscus calcification and the severity of cartilage damage ($r = 0.925$, $P < .0001$ and $r = 0.944$, $P < .0001$, respectively) (Figure 3C).

Expression of Typical Hypertrophic and Mineralization Markers in the Meniscus—Immunohistochemistry was performed to determine the presence of MMP-13, Col X, Ihh, IL-1, ANKH, ENPP1, and ALP in the control and ACLT menisci (Figure 4, A and B). The percentages of positive expression areas of the hypertrophic markers, Ihh, MMP-13, and Col X, and the mineralization markers, ANKH, ENPP1, and ALP, were increased in the ACLT animals compared with the controls (Figure 4C).

PPi and Pi Concentrations in the Meniscus—ELISA further confirmed that the ACLT animals had higher PPi and Pi concentrations than the control animals ($P < .05$) (Figure 3D, a and b). The Pi/PPi ratio in the ACLT group (1.7) was much higher than that in

the control group (1.2) (P <.05) (Figure 3D, c), which correlated with histological calcification found in the meniscus after an ACL injury.

In Vitro Bovine Meniscus Explant Study

Cyclic Impact Loading and Cell Viability In Vitro—Live/dead staining showed that there was no obvious cell death in 1- and 2-hour loaded samples (Figure 4C, c and d) and only minor cell death in the superficial zone of 3-hour loaded bovine meniscus explants (Figure 4C, e). The meniscus explants showed cell death (red) in the positive control samples (Figure 4C, b) and no cell death in the no loading samples (Figure 4C, a).

Increased GAG Release and PPi and Pi Concentrations in the Culture Medium—An increase in GAG release in the culture medium was detected in the 48-hour samples by 19% (P < .05) and 72-hour samples by 17% (P < .05). However, there were no significant changes in the 24-hour samples compared with the control group (Figure 5A).

The concentrations of PPi and Pi were significantly increased in the 3-hour loaded explants after 72 hours by 13% and 30%, respectively, compared with the control group by ELISA (Figure 5B, a and b). No significant changes were detected in the 24- and 48-hour samples. The Pi/PPi ratio was increased in 3-hour loaded samples compared to the control group cultured for 72 hours (P < .05) (Figure 5B, c).

Gene and Protein Changes Associated With Hypertrophy and Mineralization After Cyclic Impact Loading—RT-qPCR analyses indicated that cyclic impact loading increased the levels of ANKH, ENPP1, and ALP mRNA in the loaded bovine meniscus explants compared with the control group (P <.05) (Figure 6A).

Representative Western blot results showed a high level of MMP-13 and ANKH proteins in 3-hour loaded explants (cultured for 24, 48, and 72 hours) when compared with the nonloaded group (P <.05) (Figure 6B, a, c, and d). Coomassie Blue staining was used to confirm equal loading (Figure 6B, b).

DISCUSSION

In this study, our data clearly demonstrate that ACLT results in significant meniscus hypertrophy in vivo in guinea pigs and increases the levels of Col X, Ihh, MMP-13, and IL-1, which are specific markers for hypertrophy. We also found an increase in pathological matrix calcification of menisci in the ACLT group by fluorescent microscopy and Alizarin Red and von Kossa staining. These findings were correlated by Western blot and RT-qPCR analysis. An increase in mineralization-related genes such as ANKH, ENPP1, and ALP resulted in an increase in the Pi/PPi ratio in our in vivo ACLT animal model. The in vivo data from the guinea pig ACLT model were further confirmed in vitro by using bovine meniscus explants exposed to mechanical loading. Previous studies have indicated that an ACL rupture results in abnormal compressive loading.[15,27] Our results suggest that abnormal compressive loading induced by an ACL injury results in meniscus hypertrophy and accelerates meniscus mineralization by up-regulating hypertrophic and mineralization-related genes.

A previous study found that meniscus calcification is positively associated with meniscus degeneration and is a predisposing factor for cartilage lesions.[35] Meniscus degeneration can reduce load transmission, shock absorption, and joint stability, and this process changes the mechanical environment of the knee joint, which may initiate cartilage damage.[35] Our regression analysis indicates that there is a strong correlation between meniscus calcification and the severity of cartilage damage. This finding is consistent with those in previous reports in which the loss of meniscus function is a risk factor for the subsequent development of knee OA because of the increased mechanical stress to the articular cartilage.[12,14,18,19] Our findings suggest that meniscus hypertrophy and mineralization may play an important role during the development of knee OA after an ACL injury. However, the exact relationship between meniscus degeneration and PTOA is complex, and the cause and effect relationship of meniscus hypertrophy and mineralization in the development of PTOA requires additional studies for full understanding.

Hypertrophy and calcification are complicated processes controlled by local as well as systemic factors. Abnormal loading increased the levels of Col X, Ihh, MMP-13, and IL-1. The markers known to induce cell hypertrophy and matrix degeneration[17,48] were present in the ACLT samples but not in healthy articular cartilage.[6,42]

The mineralization process involves a balance between the local mineralization promoter(s) and its inhibitor(s). PPi and Pi are critical factors in the balance of mineralization.[26] PPi is known to potently inhibit the nucleation and propagation of basic calcium phosphate crystals.[39] Pi is a major component of hydroxyapatite (HA) crystals and serves to promote mineralization via the formation and deposition of HA in a forming or propagating mineralization front.[26] PPi and Pi are influenced by manifold factors including ANKH, ENPP1, and ALP. ANKH regulates extracellular PPi steady-state concentrations by transporting PPi to the extracellular microenvironment.[46] ENPP1 increases the extracellular PPi concentration to effectively inhibit HA crystals and plays a significant role in regulating physiological and pathological tissue mineralization.[33] ALP increases Pi concentrations by cleaving PPi.[21] All of these mineralization genes were up-regulated after ACL injuries. We showed that the Pi/PPi ratio was significantly increased in ACLT animals, and we believe that explains why more mineralization was found in the ACLT animals compared with the control group. Our findings are consistent with those of 34 previous studies in which pathological calcification is universally present in hyaline articular cartilage and the meniscus of patients with OA.[2,19,35] Recent studies showed that 80% of the knees affected by meniscus calcification had associated cartilage lesions as compared with 35% of the knees without meniscus calcification in age-matched patients.[28,29] Time-course studies in animals indicated that meniscus calcification occurred before cartilage breakdown.[35] A positive correlation between meniscus calcification and cartilage lesions has also been noted in animal OA models including mice, cats, and Hartley guinea pigs.[35] These findings indicate that calcification induced by abnormal loading after ACLT is an early event in the disease process and a predisposing factor for articular cartilage lesions.

Cell death in the surface layer was detected in the superficial zone of the bovine meniscus explants after 3 hours of loading. Cell death is an early event in tissue trauma and is an important feature in tissue damage.[16] We used 25% strain at 0.3 Hz for our in vitro

study.[40,49] We found that the dynamic compressive strains induced GAG release and up-regulated the expression of genes and proteins related to hypertrophy and mineralization, including MMP-13, ANKH, ENPP1, and ALP. Our data are consistent with previous findings in which dynamic compressive strains on meniscus explants increased GAG release from tissue and induced IL-1α.[50] A similar result was also reported in rat end-plate chondrocytes.[46] Our in vitro and in vivo evidence indicates that abnormal mechanical loading after ACLT can promote and accelerate meniscus hypertrophy and mineralization.

Our research study has several limitations. One limitation is the possible interaction between primary and secondary OA in the animals employed. Several studies reported that Hartley guinea pigs begin to develop mild OA by 9 months of age through natural aging.[7,8,44,45] In our study, the secondary OA model was superimposed on the primary OA model by performing ACLT at 3 months. The animals were sacrificed when they were 5.5 months old. However, this should not be a major concern, given the differences in the magnitude found in the histology, gene changes, and mineralization of the ACLT knee compared with the contralateral control knee after such a short duration. Second, this study was performed in guinea pigs, and it is unclear if these changes would be the same in human PTOA after ACL ruptures. However, “an end-stage sample” from a patient undergoing joint replacement surgery for the treatment of OA showed pathological calcification in hyaline cartilage and the meniscus.[24] It would be interesting to know whether there is a difference regarding pathological calcification between human PTOA after ACL ruptures and “idiopathic” OA in a future study. Third, we did not test the biomechanical properties of the knee meniscus after ACL injuries nor relate the biomechanics to changes in hypertrophy and mineralization, which should be done in a future study. Finally, another limitation is that a better control would be sham surgery in another animal as the load transfer to the contralateral limb could alter metabolic effects.

CONCLUSION

Our results indicate that ACL injuries in vivo and abnormal loading in vitro result in the overexpression of several important genes and proteins involved in hypertrophy and mineralization. In the meniscus, hypertrophy and calcification are early events that correlate to the magnitude of cartilage damage in PTOA. Our data imply that the suppression of meniscus hypertrophy and calcification may be an additional target for the prevention of PTOA.

Acknowledgments

The authors also gratefully acknowledge Linghui Li, Huihao Wang, and Xianwen Shang for assistance with quantifying the cartilage damage score and meniscus grade.

References

1. Ajuied A, Wong F, Smith C, et al. Anterior cruciate ligament injury and radiologic progression of knee osteoarthritis: a systematic review and meta-analysis. Am J Sports Med. 2014; 42(9):2242–2252. [PubMed: 24214929]
2. Ali SY. Apatite-type crystal deposition in arthritic cartilage. Scan Electron Microsc. 1985; (Pt 4): 1555–1566. [PubMed: 4095501]

3. Atarod M, Frank CB, Shrive NG. Increased meniscal loading after anterior cruciate ligament transection in vivo: a longitudinal study in sheep. Knee. 2015; 22(1):11–17. [PubMed: 25487300]
4. Baker P, Coggon D, Reading I, Barrett D, McLaren M, Cooper C. Sports injury, occupational physical activity, joint laxity, and meniscal damage. J Rheumatol. 2002; 29(3):557–563. [PubMed: 11908573]
5. Bilgen B, Chu D, Stefani R, Aaron RK. Design of a biaxial mechanical loading bioreactor for tissue engineering. J Vis Exp. 2013; (74):e50387. [PubMed: 23644779]
6. Brew CJ, Clegg PD, Boot-Handford RP, Andrew JG, Hardingham T. Gene expression in human chondrocytes in late osteoarthritis is changed in both fibrillated and intact cartilage without evidence of generalised chondrocyte hypertrophy. Ann Rheum Dis. 2010; 69:234–240. [PubMed: 19103633]
7. Bri E, Lei W, Reinholt FP, Mengarelli-Widholm S, Heingård D, Svensson O. Ultrastructural immunolocalization of bone sialoprotein in guinea-pig osteoarthritis. Osteoarthritis Cartilage. 1997; 5(6):387–393. [PubMed: 9536287]
8. Brismar BH, Lei W, Hjerpe A, Svensson O. The effect of body mass and physical activity on the development of guinea pig osteoarthrosis. Acta Orthop Scand. 2003; 74(4):442–448. [PubMed: 14521296]
9. Chalmers PN, Mall NA, Moric M, et al. Does ACL reconstruction alter natural history? A systematic literature review of long-term outcomes. J Bone Joint Surg Am. 2014; 96:292–300. [PubMed: 24553885]
10. Chan WP, Lang P, Stevens MP, et al. Osteoarthritis of the knee: comparison of radiography, CT, and MR imaging to assess extent and severity. AJR Am J Roentgenol. 1991; 157(4):799–806. [PubMed: 1892040]
11. Chen CT, Burton-Wurster N, Borden C, Hueffer K, Bloom SE, Lust G. Chondrocyte necrosis and apoptosis in impact damaged articular cartilage. J Orthop Res. 2001; 19(4):703–711. [PubMed: 11518282]
12. Cui X, Hasegawa A, Lotz M, D'Lima D. Structured three-dimensional co-culture of mesenchymal stem cells with meniscus cells promotes meniscal phenotype without hypertrophy. Biotechnol Bioeng. 2012; 109(9):2369–2380. [PubMed: 22422555]
13. Dare D, Rodeo S. Mechanisms of post-traumatic osteoarthritis after ACL injury. Curr Rheumatol Rep. 2014; 16(10):448. [PubMed: 25182676]
14. Felson DT, Zhang Y. An update on the epidemiology of knee and hip osteoarthritis with a view to prevention. Arthritis Rheum. 1998; 41:1343–1355. [PubMed: 9704632]
15. Fithian DC, Paxton EW, Stone ML, et al. Prospective trial of a treatment algorithm for the management of the anterior cruciate ligament-injured knee. Am J Sports Med. 2005; 33(3):335–346. [PubMed: 15716249]
16. Ho JO, Sawadkar P, Mudera V. A review on the use of cell therapy in the treatment of tendon disease and injuries. J Tissue Eng. 2014; 5:2041731414549678. [PubMed: 25383170]
17. Hufeland M, Schünke M, Grodzinsky AJ, Imgenberg J, Kurz B. Response of mature meniscal tissue to a single injurious compression and interleukin-1 in vitro. Osteoarthritis Cartilage. 2013; 21(1):209–216. [PubMed: 23069857]
18. Hunter DJ, Zhang YQ, Niu JB, et al. The association of meniscal pathologic changes with cartilage loss in symptomatic knee osteoarthritis. Arthritis Rheum. 2006; 54(3):795–801. [PubMed: 16508930]
19. Johnson K, Pritzker K, Goding J, Terkeltaub R. The nucleoside tri-phosphate pyrophosphohydrolase isozyme PC-1 directly promotes cartilage calcification through chondrocyte apoptosis and increased calcium precipitation by mineralizing vesicles. J Rheumatol. 2001; 28(12):2681–2691. [PubMed: 11764218]
20. Jørgensen SH, Rasmussen C, Espesen J. Cholesterol crystals in synovial fluid in patients with rheumatoid arthritis may be linked with a poor prognosis [in Danish]. Ugeskr Laeger. 2014; 176(46):V06140378. [PubMed: 25394926]
21. Kaji H. Pyrophosphate and mineralization. Clin Calcium. 2007; 17(10):1574–1579. [PubMed: 17906411]

22. Kraus VB, Huebner JL, DeGroot J, Bendele A. The OARSI histopathology initiative: recommendations for histological assessments of osteoarthritis in the guinea pig. Osteoarthritis Cartilage. 2010; 18(Suppl 3):S35–S52. [PubMed: 20864022]
23. Li S, Blain EJ, Cao J, Caterson B, Duance VC. Effects of the mycotoxin nivalenol on bovine articular chondrocyte metabolism in vitro. PLoS One. 2014; 9(10):e109536. [PubMed: 25329658]
24. MacMullan PA, McCarthy GM. The meniscus, calcification and osteoarthritis: a pathologic team. Arthritis Res Ther. 2010; 12(3):116. [PubMed: 20500910]
25. Mäkelä JT, Rezaeian ZS, Mikkonen S, et al. Site-dependent changes in structure and function of lapine articular cartilage 4 weeks after anterior cruciate ligament transection. Osteoarthritis Cartilage. 2014; 22(6):869–878. [PubMed: 24769230]
26. Matsuo K. Updates on rickets and osteomalacia: mechanism and regulation of bone mineralization. Clin Calcium. 2013; 23(10):1463–1467. [PubMed: 24076644]
27. Meyer EG, Baumer TG, Slade JM, Smith WE, Haut RC. Tibiofemoral contact pressures and osteochondral microtrauma during anterior cruciate ligament rupture due to excessive compressive loading and internal torque of the human knee. Am J Sports Med. 2008; 36(10):1966–1977. [PubMed: 18490469]
28. Mitrovic D, Stankovic A, Morin J, et al. Anatomic incidence of menis-cochondrocalcinosis of the knee. Rev Rhum Mal Osteoartic. 1982; 49(7):495–499. [PubMed: 6896928]
29. Mitrovic DR, Stankovic A, Iriarte-Borda O, et al. The prevalence of chondrocalcinosis in the human knee joint: an autopsy survey. J Rheumatol. 1988; 15(4):633–641. [PubMed: 3397973]
30. Quatman CE, Kiapour AM, Demetropoulos CK, et al. Preferential loading of the ACL compared with the MCL during landing: a novel in sim approach yields the multiplanar mechanism of dynamic valgus during ACL injuries. Am J Sports Med. 2014; 42(1):177–186. [PubMed: 24124198]
31. Rijk PC, Tigchelaar-Gutter W, Bernoski FP, Van Noorden CJ. Histologic changes in articular cartilage after medial meniscus replacement in rabbits. Arthroscopy. 2004; 20(9):911–917. [PubMed: 15525923]
32. Rue J-P, Kilcoyne K, Dickens J. Complex knee problems in a young, active duty military population, part I: ACL reconstruction, allograft OATS, and treatment of meniscal injuries. J Knee Surg. 2011; 24(2):71. [PubMed: 21874941]
33. Rutsch F, Vaingankar S, Johnson K, et al. PC1 nucleoside triphosphate pyrophosphohydrolase deficiency in idiopathic infantile arterial calcification. Am J Pathol. 2001; 158(2):543–554. [PubMed: 11159191]
34. Ryu JH, Provencher MT. Special considerations for ACL graft selection in the young, active military patient. J Knee Surg. 2011; 24(2):73–82. [PubMed: 21874942]
35. Sun Y, Mauerhan DR. Meniscal calcification, pathogenesis and implications. Curr Opin Rheumatol. 2012; 24(2):152–157. [PubMed: 22227878]
36. Sun Y, Mauerhan DR, Honeycutt PR, et al. Analysis of meniscal degeneration and meniscal gene expression. BMC Musculoskelet Disord. 2010; 11:19. [PubMed: 20109188]
37. Sun Y, Mauerhan DR, Honeycutt PR, et al. Calcium deposition in osteoarthritic meniscus and meniscal cell culture. Arthritis Res Ther. 2010; 12(2):R56. [PubMed: 20353559]
38. Tambutté E, Tambutté S, Segonds N, et al. Calcein labelling and electrophysiology: insights on coral tissue permeability and calcification. Proc Biol Sci. 2012; 279(1726):19–27. [PubMed: 21613296]
39. Terkeltaub RA. Inorganic pyrophosphate generation and disposition in pathophysiology. Am J Physiol Cell Physiol. 2001; 281(1):C1–C11. [PubMed: 11401820]
40. Upton ML, Chen J, Guilak F, Setton LA. Differential effects of static and dynamic compression on meniscal cell gene expression. J Orthop Res. 2003; 21(6):963–969. [PubMed: 14554206]
41. Vignery A, Baron R. Dynamic histomorphometry of alveolar bone remodeling in the adult rat. Anat Rec. 1980; 196(2):191–200. [PubMed: 7416512]
42. Wang X, Manner PA, Horner A, Shum L, Tuan RS, Nuckolls GH. Regulation of MMP-13 expression by RUNX2 and FGF2 in osteoarthritic cartilage. Osteoarthritis Cartilage. 2004; 12:963–973. [PubMed: 15564063]

43. Wei F, Zhou J, Wei X, et al. Activation of Indian hedgehog promotes chondrocyte hypertrophy and upregulation of MMP13 in human osteoarthritic cartilage. Osteoarthritis Cartilage. 2012; 20(7): 755–763. [PubMed: 22469853]
44. Wei L, Svensson O, Hjerpe A. Correlation of morphological and biochemical changes in the natural history of the spontaneous osteoarthrosis in guinea pigs. Arthritis Rheum. 1997; 40(11): 2075–2083. [PubMed: 9365098]
45. Wei L, Svensson O, Hjerpe A. Proteoglycan turnover during development of spontaneous osteoarthrosis in guinea pigs. Osteoarthritis Cartilage. 1998; 6(6):410–416. [PubMed: 10343774]
46. Xu HG, Hu CJ, Wang H, et al. Effects of mechanical strain on ANK, ENPP1 and TGF-β1 expression in rat end plate chondrocytes in vitro. Mol Med Rep. 2011; 4(5):831–835. [PubMed: 21674130]
47. Yu JW, Duan WJ, Huang XR, et al. MicroRNA-29b inhibits peritoneal fibrosis in a mouse model of peritoneal dialysis. Lab Invest. 2014; 94(9):978–990. [PubMed: 25046436]
48. Zhang C, Wei X, Chen C, et al. Indian hedgehog in synovial fluid is a novel marker for early cartilage lesions in human knee joint. Int J Mol Sci. 2014; 15(5):7250–7265. [PubMed: 24786088]
49. Zielinska B, Donahue TL. 3D finite element model of meniscectomy: changes in joint contact behavior. J Biomech Eng. 2006; 128(1):115–123. [PubMed: 16532624]
50. Zielinska B, Killian M, Kadmiel M, Nelsen M, Haut Donahue TL. Meniscal tissue explants response depends on level of dynamic compressive strain. Osteoarthritis Cartilage. 2009; 17(6): 754–760. [PubMed: 19121588]

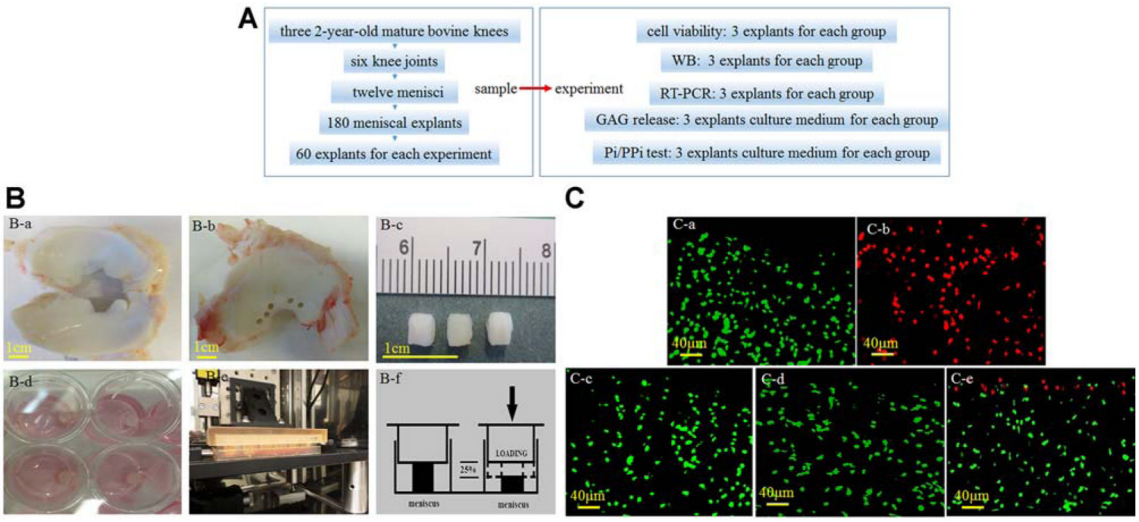

Figure 1.

Cyclic impact loading and cell viability in meniscus explants. (A) The numbers of animals, joints, menisci, explants, and experimental designs in the bovine meniscus explant study. (B) The meniscus explants (a–c) were subjected to a loading injury by indenting to 25% strain at 0.3 Hz for 1, 2, and 3 hours (d–f). (C) Green fluorescence indicates living cells, and red fluorescence indicates dead cells. No cell deaths were detected in the (a) no loading, (c) 1-hour loading, or (d) 2-hour loading samples, and (b) all cells were dead in the freeze-thawed samples. (e) A single layer of cell death was detected in the superficial zone of 3-hour loaded bovine meniscus explants.

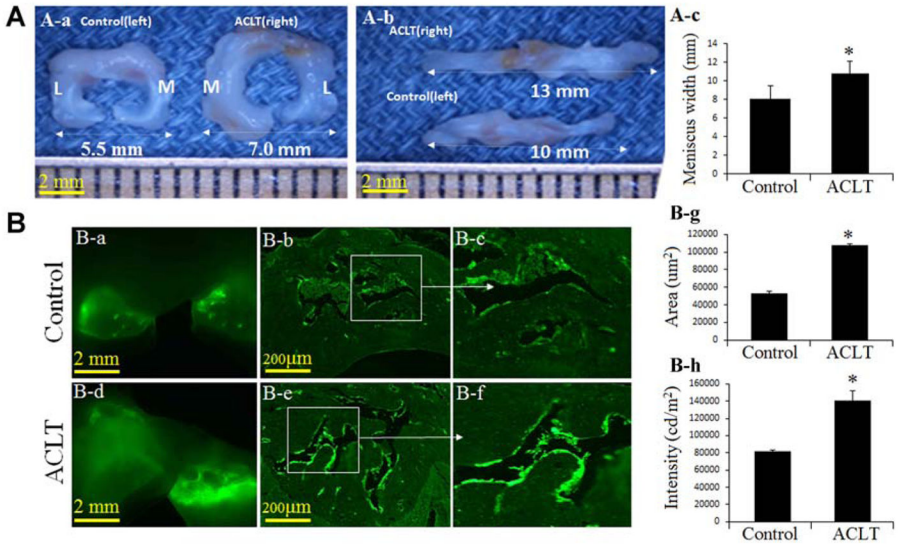

Figure 2.

Abnormal loading results in meniscus hypertrophy and accelerates pathological matrix calcification after an ACL injury. (A) (a) The width between the lateral meniscus and medial meniscus, (b) the meniscus length, and (c) bar graphs showing the mean size from medial to lateral. (B) Fluorescent microscopy images show an increase in pathological matrix calcification in the (a, d) whole meniscus tissue and (b, detail c, e, and detail f) ACL-transected (ACLT) group; bar graphs (g, h) show the area and intensity of pathological matrix calcification in meniscus tissue of the ACLT group compared with controls (n = 3; **P* < .05 compared with controls). L, lateral; M, medial.

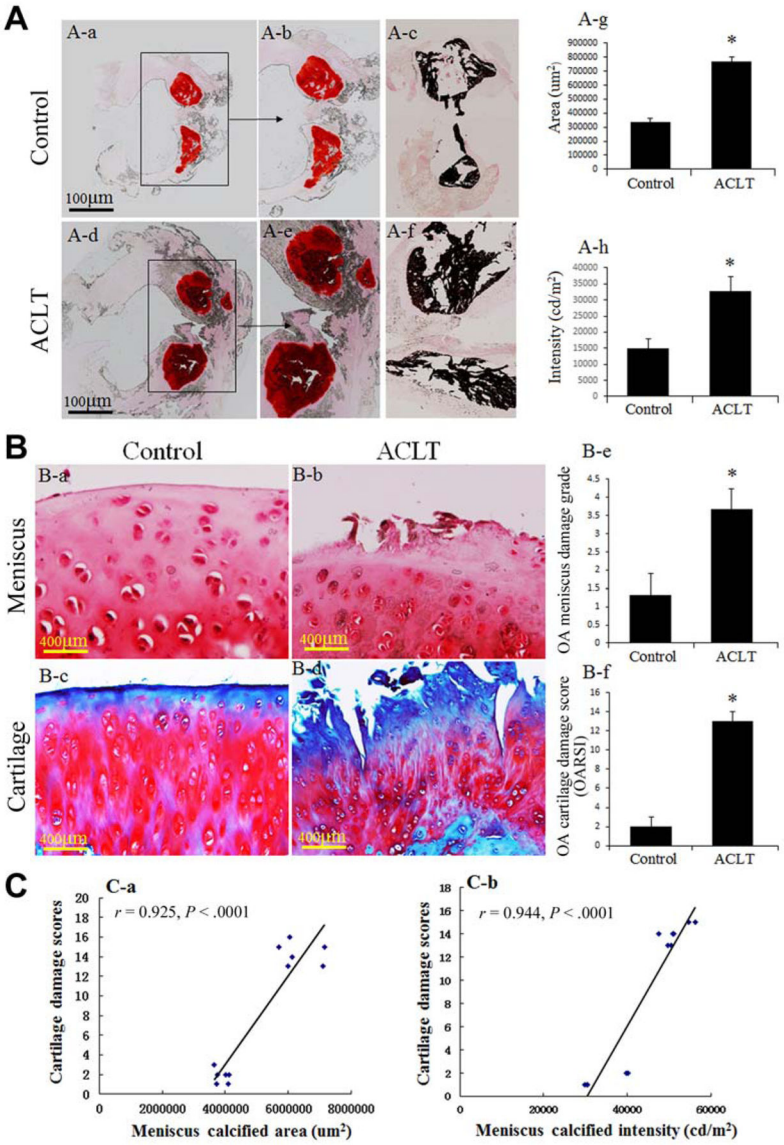

Figure 3.

Anterior cruciate ligament (ACL) injuries accelerated meniscus calcification and correlated with cartilage damage. (A) (a, b, d, e) Alizarin Red and (c, f) von Kossa staining indicate strong calcification in the ACL-transected (ACLT) animals compared with controls. (g, h) Bar graphs show the area and intensity of meniscus calcification (n = 3; **P* <.05). (B) Safranin O staining shows damage to the (a, b) anterior horn of the medial meniscus and (c, d) cartilage of the proximal tibial plateau in the ACLT animals relative to controls. (e, f) Bar graphs depict the meniscus grade and Osteoarthritis Research Society International (OARSI) score (n = 3; **P* <.05). (C) Significant correlations were found between the area and intensity of meniscus calcification and the severity of cartilage damage (n = 6; **P* <.05 compared with controls).

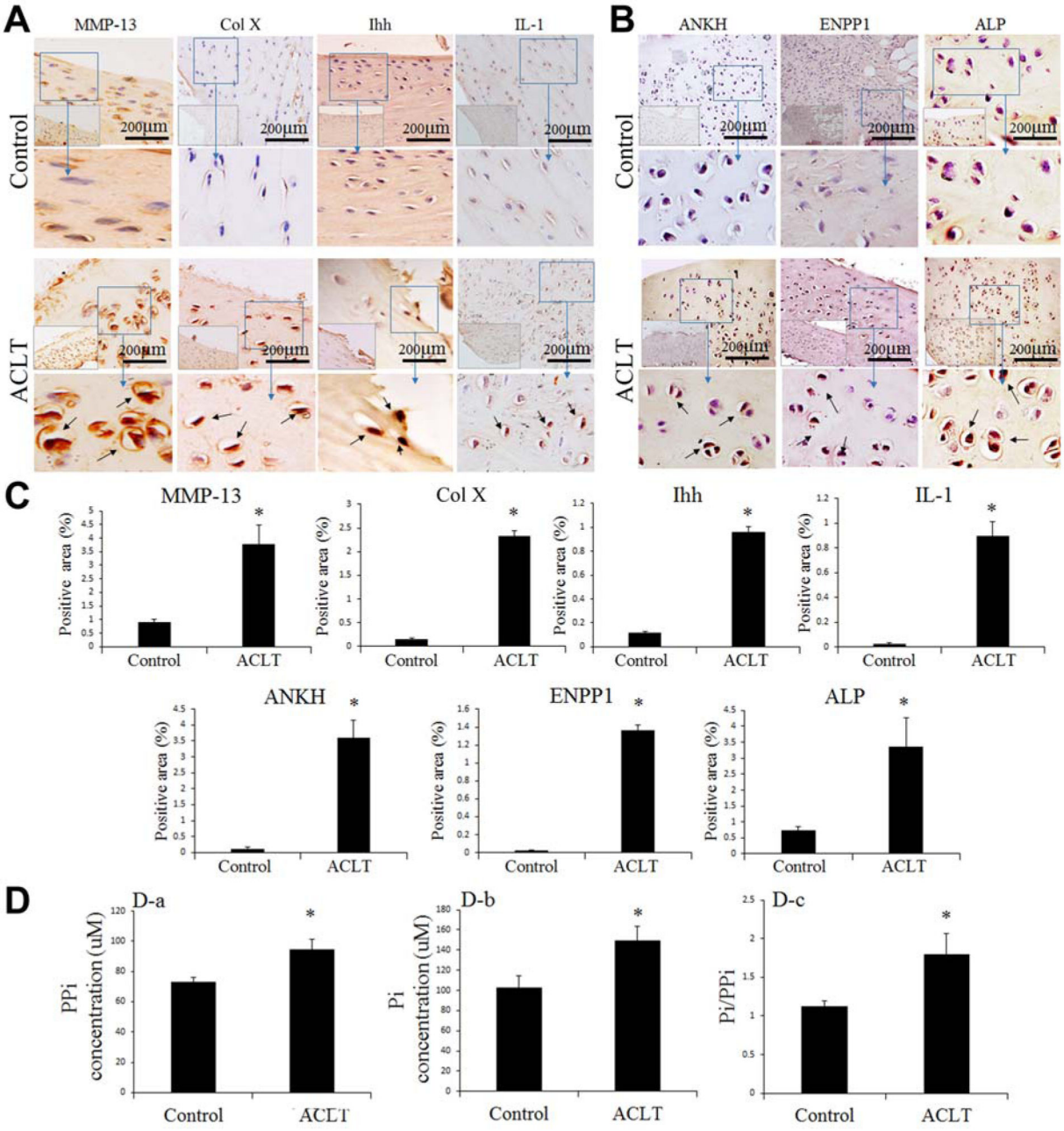

Figure 4.

Increases in MMP-13, Col X, Ihh, IL-1, ANKH, ENPP1, ALP, PPi, and Pi concentrations were found in the ACLT meniscus group. Immunohistochemistry staining: (A) Ihh, MMP-13, Col X, IL-1 and (B) ANKH, ENPP1, ALP. Positive signals (brown staining) are indicated by arrows. (C) Semiquantitative analysis of Ihh, MMP-13, Col X, IL-1, ANKH, ENPP1, ALP-positive expression area. (D) Bar graphs show: (a, b) PPi and Pi concentrations and (c) Pi/PPi ratio in the ACLT and control groups (n = 3; **P* <.05 compared with controls). ACLT, anterior cruciate ligament–transected; ALP, alkaline phosphatase; ANKH, progressive ankylosis homolog; Col X, collagen type X; ENPP1,

ectonucleotide pyrophosphatase/phosphodiesterase–1; Ihh, Indian hedgehog; IL-1, interleukin-1; MMP-13, matrix metalloproteinase–13; Pi, inorganic phosphate; PPi, inorganic pyrophosphate.

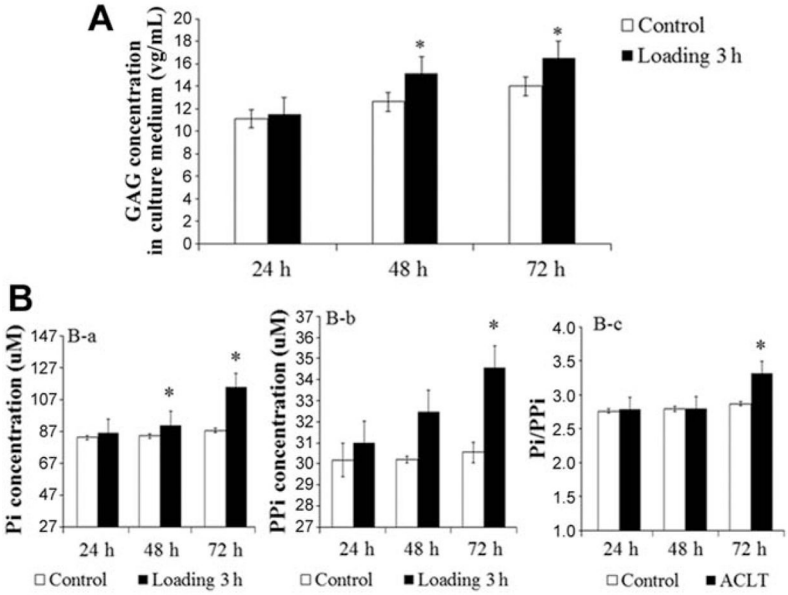

Figure 5.

Increased GAG release and PPi and Pi concentrations in the explant culture medium. (A) Spectrophotometry analysis demonstrated no increase in GAG release in the cultured medium from 3-hour loaded samples at 24 hours after culture (n = 3), but it increased by 19% and 17% in 48- and 72-hour samples, respectively, compared with the control group (n = 3; **P* <.05 compared with controls). (B) Bar graphs show the concentration of (a) Pi, (b) PPi, and (c) Pi/PPi ratio in the culture medium from 3-hour loaded samples after 24-, 48-, and 72-hour cultures, respectively, and the control group (n = 3; **P* <.05 compared with controls). GAG, glycosaminoglycan; Pi, inorganic phosphate; PPi, inorganic pyrophosphate.

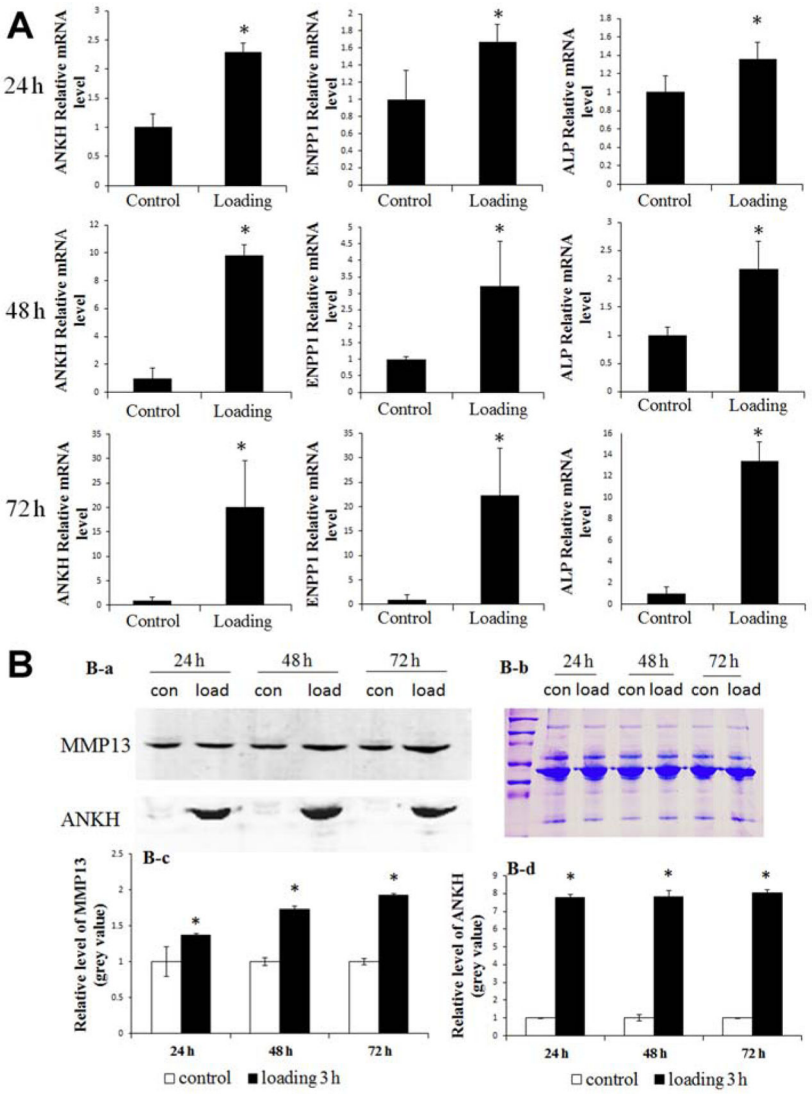

Figure 6.

Increase in ANKH, ENPP1, and ALP mRNA and MMP-13 and ANKH proteins from 3-hour loaded explants after culture for 24, 48, and 72 hours after loading compared with the control group. (A) Bar graphs show the mean quantified data of ANKH, ENPP1, and ALP mRNA from 3 independent experiments (n = 3; **P* <.05). (B) (a) The protein levels of MMP-13 and ANKH were detected by Western blot. (b) Coomassie Blue staining was used to confirm equal loading. (c, d) Bar graphs show the mean quantified data of MMP-13 and ANKH proteins from 3 independent experiments (n = 3; **P* <.05 compared with controls). ALP, alkaline phosphatase; ANKH, progressive ankylosis homolog; ENPP1, ectonucleotide pyrophosphatase/phosphodiesterase–1; MMP-13, matrix metalloproteinase–13.